

Determination of Secondary Structural Changes in Gluten Proteins during Mixing Using Fourier Transform Horizontal Attenuated Total Reflectance Spectroscopy

BRADFORD W. SEABOURN,^{*,†} OKKYUNG K. CHUNG,[†] PAUL A. SEIB,[‡] AND
PAUL R. MATHEWSON[§]

Grain Marketing & Production Research Center, Agricultural Research Service, U.S. Department of Agriculture, Manhattan, Kansas 66502, Department of Grain Science & Industry, Kansas State University, Shellenberger Hall, Manhattan, Kansas 66506, and The Food Technology Resource Group, 7726 Buckboard Drive, Park City, Utah 84060

Fourier transform horizontal attenuated total reflectance (FT-HATR) was used to examine changes in the secondary structure of gluten proteins in a flour–water dough system during mixing. Midinfrared spectra of mixed dough revealed changes in four bands in the amide III region associated with secondary structure in proteins: 1317 (α -helix), 1285 (β -turn), 1265 (random coil), and 1242 cm^{-1} (β -sheet). The largest band, which also showed the greatest change in second derivative band area (SDBA) during mixing, was located at 1242 cm^{-1} . The bands at 1317 and 1285 cm^{-1} also showed an increase in SDBA over time. Conversely, the band at 1265 cm^{-1} showed a corresponding decrease over time as the doughs were mixed. All bands reached an optimum corresponding to the minimum mobility of the dough as determined by the mixograph. Increases in α -helix, β -turn, and β -sheet secondary structures during mixing suggest that the dough proteins assume a more ordered conformation. These results demonstrate that it is possible, using infrared spectroscopic techniques, to relate the rheological behavior of developing dough in a mixograph directly to changes in the structure of the gluten protein system.

KEYWORDS: Attenuated total reflectance; secondary structure; amide III; rheology

INTRODUCTION

Dough Rheology. The mixing of dough, and the point at which it reaches optimum hydration and development, has typically been a process of visual and tactile assessment of the dough mass (color, texture, consistency, and stickiness) or its response to work input via the mixograph, farinograph, or other such devices. While these practices have adequately served industry and researchers for many years, they are largely subjective in nature. More objective methods for measuring the development of dough systems, preferably methods based on the chemical characteristics of dough component interaction(s), have long been desired by cereal chemists.

It is generally recognized that when flour and water are optimally mixed, at least three things are accomplished as follows: (i) a homogeneous mass of flour and water is formed, (ii) a three-dimensional protein network is developed with the unique capacity to hold gas, and (iii) air cells are incorporated

into the dough. When water is added to flour and the mixing process is started, flour protein absorbs water and partially unfolds due to the shear and tensile forces imparted to the dough as a result of the mixing process (1–6). It is believed that hydrophobic interactions and sulfhydryl–disulfide interchange reactions allow threadlike polymers to form in the presence of water (7). These polymers are then thought to interact with each other through hydrogen bonding, additional hydrophobic interactions, sulfhydryl–disulfide interchanges, and physical entanglements created during the mixing process to form a continuous sheetlike film of protein with the unique ability to retain fermentation gases (8–10).

As the undeveloped dough continues to mix, resistance to work input increases until a maximum (point of minimum mobility) or optimum mix time is reached that is physically indicative of maximum hydration of flour components and best possible development of a continuous gluten network. The time required to reach optimum development, as well as sustained resistance to work input beyond optimum, are used as factors in measuring flour quality for bread making. It is believed that continued mixing beyond the point of minimum mobility results in a breakdown of the continuous gluten network through

* To whom correspondence should be addressed. Tel: 785-776-2751. Fax: 785-537-5534. E-mail: brad.seabourn@ars.usda.gov.

[†] U.S. Department of Agriculture.

[‡] Kansas State University.

[§] The Food Technology Resource Group.

alignment of protein polymers in the direction of shear, as well as the rupture of potential disulfide cross-links and the ultimate reduction in molecular weight of gluten polymers (11–13).

Infrared Spectroscopic Analysis. Fourier transform infrared (FT-IR) spectroscopy has undergone a renaissance in the last 10–15 years with major improvements and revolutionary changes in spectrometer components, more affordable instrumentation, and the advent of very fast and powerful personal computers. As a result, the use of FT-IR in biological applications, particularly in the characterization of proteins, has increased at an unprecedented rate.

The primary basis for the study of proteins using infrared spectroscopy is that the infrared signatures of proteins are unique and provide a means for spectroscopists to “fingerprint” protein composition and structure (14). The structural repeat unit of proteins, the peptide group, gives nine characteristic mid-infrared (mid-IR) bands, named amides A, B, and I–VII. The amide I (1700–1600 cm^{-1}) and II (1600–1500 cm^{-1}) bands are two major bands of the protein infrared spectrum and have traditionally been used to characterize protein structure. The amide I region (1700–1600 cm^{-1}) corresponds to the C=O stretch vibration and is directly related to the (poly)peptide backbone of the protein molecule. The amide II region (1600–1500 cm^{-1}) represents C–N stretch strongly coupled with N–H bending and is sensitive to conformational changes in protein structure. The amide III region (1350–1200 cm^{-1}) corresponds to N–H in-plane bending (40–60%) coupled with C–N stretching (18–40%) and also includes C–H and N–H deformation vibrations (15).

Fundamental to the present study is the work of Singh et al. (16) and Shuwei and Singh (17), which demonstrated the utility of using the amide III region of the mid-IR for estimating secondary structures in the proteins. The authors showed that although the signal is weaker in the amide III, this region offered several advantages, the most important being that water vibrations (–OH) do not interfere with the protein spectrum as in the amide I, eliminating the need for tedious and time-consuming hydrogen–deuterium exchange techniques or spectral subtraction errors to resolve protein peaks. In addition, secondary structures such as α -helix, β -sheet, and random coil are more localized in the amide III and do not overlap as much as they do in the amide I, resulting in less ambiguity of band assignment. In many cases, peaks in the amide III are visualized before any other processing or statistical methods are applied. Cai and Singh (18) further established band assignments in the amide III for α -helix (1330–1295 cm^{-1}), β -sheet (1245–1220 cm^{-1}), β -turn (1295–1270 cm^{-1}), and random coil (1270–1255 cm^{-1}).

Essential to protein characterization is the requirement that some estimate of its secondary structure be made. Early work by Mathewson (19) established criteria for estimating the secondary structure of proteins using FT-IR spectroscopy, and many other researchers have since established FT-IR spectroscopy as a viable method for evaluating and estimating the conformation and conformational changes in proteins (16, 17, 20–28). The work of Pezolet et al. (29) introduced FT-IR as a tool for analyzing wheat gluten proteins, as well as their functional and hydrated states in dough. These authors also initiated attenuated total reflectance (ATR) as a useful technique for evaluating gluten proteins. Seabourn (30) expanded this research further with the first study of conformational changes in gluten proteins in dough systems under work input.

Recent work has been conducted in the mid-infrared by Wellner et al. (31) using ATR spectroscopy in the study of gluten protein. Band shifts in the amide I and II measurements

of hydrated gluten under applied deformation caused an increase in intermolecular β -sheet structures at the expense of β -turn and α -helix structures. More recently, Bruun et al. (32, 33) studied gluten protein conformation in dry and hydrated states and confirmed observed changes in near-infrared protein bands, which could be explained by changes in protein secondary structure and water-binding abilities.

The objective of this study was to use Fourier transform horizontal ATR (FT-HATR) to provide direct evidence that flour protein in the presence of water undergoes a change in secondary structure during mixing, to identify the secondary structures involved, and to determine how these structures relate to the rheological properties of the dough as it develops by means of mechanical mixing.

MATERIALS AND METHODS

Flour Samples. Straight grade flour at 13.0% protein content (14% moisture basis), 72.1% gluten (protein based), and 0.46% starch (protein based), which were initially used for the determination of bands associated with secondary structural changes in dough protein, were obtained from Midwest Grain Products Inc. (MWG) (Atchison, KS). The gluten and starch fractions were isolated from the same straight grade flour used in this study. The flour moisture content was determined by air oven, and protein contents were determined by nitrogen combustion according to America Association of Cereal Chemists (AACC) Methods 44-15A and 46-30, respectively (34).

Straight grade flour samples varying in optimum mix time (MT) and protein content (PC) were obtained from the Wheat Quality Council (WQC) for the 2000 and 2001 crop years. These flours were derived from wheat samples that were experimental lines grown at single locations. Six samples from the WQC were then selected based on PC (H = high or L = low) and MT (S = short, M = medium, or L = long). The six samples were then split into two groups (group I = HL, HM, and HS and group II = LL, LM, and LS) with three samples each. The “high” PC flours (group I) had 13.5, 14.1, and 13.9% PC, respectively (\bar{x} = 13.8%, SD = 0.3), while the “low” PC flours (group II) had 11.8, 11.4, and 11.9% PC, respectively (\bar{x} = 11.7%, SD = 0.2). Optimum MTs for the high PC flours were 2.25 (S = short), 4.38 (M = medium), and 6.00 (L = long) min, respectively, while MTs for the low PC flours were 2.50 (S = short), 4.63 (M = medium), and 6.38 (L = long) min, respectively. The optimum MT for each flour was determined by an experienced mixograph technician according to AACC Method 54-40A (34).

Dough Sample Preparation. Doughs for FT-HATR spectral analysis were prepared according to AACC Method 54-40A (34), in which 10 ± 0.001 g of flour (moisture basis, mb) was weighed and placed in a mixograph bowl at room temperature (21.5 ± 1 °C). Deionized–distilled water (dH₂O) (approximately 6.0 ± 0.01 mL, depending on the optimum requirement), also at room temperature, was then added to the flour, and the mixing process started. The optimum water absorption (WA) requirement of all test flours was predetermined by an experienced operator utilizing a 10 g mixograph (National Mfg., Lincoln, NE) at the Hard Winter Wheat Quality Laboratory (HWWQL) (Manhattan, KS). The first dough was mixed for 1 min and then carefully removed from the mixer. The dough sample was positioned on a clean, dry, ZnSe FT-HATR cell with minimal stress to the dough and then scanned using the interferometer. After scanning, the FT-HATR sample cell was removed, wiped clean with a fine damp cloth followed by a thorough cleaning with methanol (Spectranal, Sigma-Aldrich Corp., St. Louis, MO) to remove dough residue, and then allowed to dry. A second dough from the same test flour was then prepared exactly as the first, mixed for one additional minute (2 min total), and then scanned. This process was again repeated, adding one additional minute to the mixing cycle in succession, until a standard 8 min mixing cycle was completed for the test flour (30). The mixogram for the final and full 8 min mixing cycle for each test flour was recorded digitally using MixSmart software version 3.80 (AEW Consulting, Lincoln, NE, commercially available through National Mfg.). This incre-

mental mix-and-scan process for the 8 min mixing cycle was then repeated twice more for the test flour sample, resulting in three replicated 8 min mixing cycles per test flour.

Infrared Measurement and Data Manipulation. A Nicolet Nexus 870 FT-IR spectrometer (Thermo Electron Corp., Madison, WI), equipped with a FT-HATR accessory (Thermo Electron Corp.), ZnSe sample cell (frequency range = 20000–650 cm^{-1} , index of refraction = 2.4), mercury–cadmium–telluride (MCT/A) liquid nitrogen-cooled detector, and a KBr beam splitter was used for recording spectra at room temperature (21.5 ± 1 °C) in the region 4000–700 cm^{-1} (30). The spectrometer was purged with CO_2 -free dry air for 24 h before recording spectra. A 128-scan coadded interferogram (mirror velocity, 1.8988; aperture, 69.00; sample gain, 1.0; Happ–Genzel apodization; and Mertz phase correction) was collected for each dough sample (one interferogram for each 1 min interval of the mixing cycle) at a resolution of 2 cm^{-1} using Thermo Electron's Omnic software (v7.3, 2006, Thermo Electron Corp.). For each dough scan, the single beam spectrum of the dough was divided by the background single beam spectrum and then converted to an absorbance spectrum. Each spectrum was manually corrected with a linear baseline correction at five points (approximately 4000, 3990, 2500, 1880, and 700 cm^{-1}), followed by an Advanced ATR Correction algorithm that further corrected for the wavelength dependence of penetration depth and refractive index dispersion around the absorbance peak (35).

Using GRAMS/AI software tools (version 7, 2001, Thermo Electron Corp.) for analyzing and processing spectral data, second derivative spectra were then obtained using a five-point, two-degree polynomial function (36), which eliminated the need for further resolution enhancement by Fourier self-deconvolution. The spectra were then smoothed with an 11-point, two-degree polynomial Savitsky–Golay function to reduce signal noise before further data analysis (37). The derivatized and smoothed spectra were individually integrated, and the second derivative band area (SDBA, in arbitrary units, AU) was calculated using the integration function within the Grams/AI software package. The zero line of the derivatized and smoothed spectra was used as the baseline for calculating the area of each relevant band within the amide III region (1350–1200 cm^{-1}). For second derivative spectra, band locations were accurately determined by inverting each spectrum (multiplying by -1), which then allowed the software to find the bands. In instances where spectral subtraction was utilized, the subtraction process was based upon removal of the band at 1339 cm^{-1} since this band was one of the largest bands in the amide III and also overlapped a band within the same region for isolated gluten. Therefore, the following criteria were used to judge the adequacy of starch subtraction: a flat baseline between 1350 and 1325 cm^{-1} (utilizing only the region between 1390 and 1220 cm^{-1} for the subtraction). Because the band at 1265 cm^{-1} (random coil) was the smallest of all the bands identified in the amide III, starch subtraction in some instances resulted in a band that was too small to integrate accurately. SDBA and peak locations (maxima) for the amide III spectral bands acquired from each scanned dough replicate in this study were recorded, and the mean and standard error (SE) for each were calculated (data not shown). The coefficient of determination (R^2) was calculated for each replicate from a point-by-point regression of the 8 min mixogram midline curve to the curve derived from changes in SDBA for a given spectral band. Replicate coefficients of determination were averaged for each spectral band, and the SE for the mean R^2 was calculated and reported (Tables 1 and 2).

RESULTS AND DISCUSSION

Secondary Structure Determination. The distinct IR spectra of proteins are the result of the differential vibrational modes of atoms in the amide bond (38). Although the amide III region is relatively narrow and does not have the signal intensity of other regions within the mid-IR typically associated with proteins, this is actually an advantage since large intense bands can be nonlinear in their response. More important to this study, the amide III region has the unique advantage of not having interfering $-\text{OH}$ vibrations from water. The amide III region (1350–1200 cm^{-1}) of water was observed to be flat and devoid

Table 1. Correlation of SDBA at 1339, 1317, and 1285 cm^{-1} to the Mixogram Midline Point for Wheat Flour with Varying PC and Optimum MT^a

sample notation ^b	PC (%)	MT (min)	wavenumber (cm^{-1})	R^2	SE ^c ($\times 10^{-4}$)
HS	13.5	2.25	1339 (α -helix)	0.83	9
HM	14.1	4.38		0.69	6
HL	13.9	6.00		0.97	4
LS	11.8	2.50		0.78	10
LM	11.4	4.63		0.90	5
LL	11.9	6.38		0.97	4
HS	13.5	2.25	1317 (α -helix)	0.80	7
HM	14.1	4.38		0.85	5
HL	13.9	6.00		0.95	3
LS	11.8	2.50		0.89	7
LM	11.4	4.63		0.99	2
LL	11.9	6.38		0.91	3
HS	13.5	2.25	1285 (β -turn)	0.72	2
HM	14.1	4.38		0.88	2
HL	13.9	6.00		0.99	1
LS	11.8	2.50		0.92	2
LM	11.4	4.63		0.98	1
LL	11.9	6.38		0.91	3

^a SDBA, second derivative band area; PC, protein content (14% mb); and MT, optimum mixogram mix time as determined by the HWWQL. ^b HS, high PC and short MT; HM, high PC and medium MT; HL, high PC and long MT; LS, low PC and short MT; LM, low PC and medium MT; and LL, low PC and long MT. ^c SE, standard error.

Table 2. Correlation of SDBA at 1265, 1242, and 1339/1242 cm^{-1} to the Mixogram Midline Point for Wheat Flours with Varying PC and Optimum MT^a

sample notation ^b	PC (%)	MT (min)	wavenumber (cm^{-1})	R^2	SE ^c ($\times 10^{-4}$)
HS	13.5	2.25	1265 (random coil)	0.85	1
HM	14.1	4.38		0.77	1
HL	13.9	6.00		0.97	1
LS	11.8	2.50		0.91	1
LM	11.4	4.63		0.95	1
LL	11.9	6.38		0.97	1
HS	13.5	2.25	1242 (β -sheet)	0.84	8
HM	14.1	4.38		0.89	8
HL	13.9	6.00		0.98	4
LS	11.8	2.50		0.69	24
LM	11.4	4.63		0.94	7
LL	11.9	6.38		0.99	3
HS	13.5	2.25	Ratio 1339/1242 (α -helix/ β -sheet)	0.88	303
HM	14.1	4.38		0.70	1210
HL	13.9	6.00		0.95	1087
LS	11.8	2.50		0.90	839
LM	11.4	4.63		0.86	1244
LL	11.9	6.38		0.95	1303

^a SDBA, second derivative band area; PC, protein content (14% mb); and MT, optimum mixogram mix time as determined by the HWWQL. ^b HS, high PC and short MT; HM, high PC and medium MT; HL, high PC and long MT; LS, low PC and short MT; LM, low PC and medium MT; and LL, low PC and long MT. ^c SE, standard error.

of any IR absorbance bands (Figure 1). The observed response for water in the 1800–1500 cm^{-1} region confirmed why the amide I and II bands of protein are difficult to resolve since they overlap with bands for water in the same region.

The spectrum of a typical adequately mixed and hydrated flour–water dough sample (Figure 1) exhibited a number of bands: a large, intense, and broad band in the region from 3815 to 2600 cm^{-1} and centered at 3410 cm^{-1} ($-\text{OH}$ stretch and free $-\text{OH}$), a smaller side band to this region centered at 2933 cm^{-1} , a third low intensity band in the region 2500–1890 cm^{-1} and centered at 2132 cm^{-1} ($-\text{OH}$), a fourth narrow and moderately intense band in the region 1800–1550 cm^{-1} and centered at 1643 cm^{-1} (amide I region) that overlaps a smaller

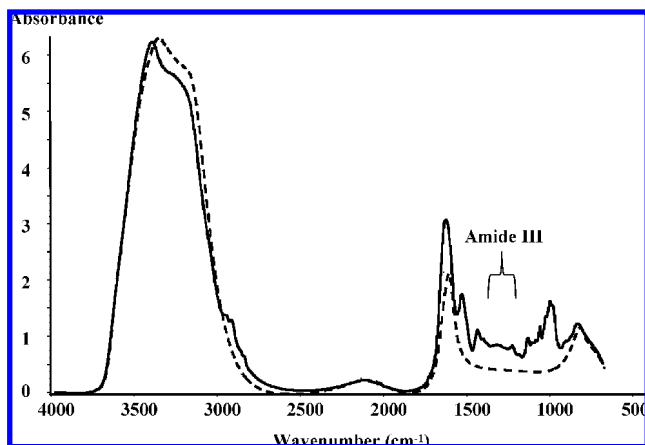


Figure 1. Raw FT-HATR spectra (baseline- and ATR-corrected) of mixed dough (solid line) and water (dashed line) in the midinfrared (4000–700 cm^{-1}).

fifth band centered at 1547 cm^{-1} in the amide II region, a sixth low intensity band centered at 1454 cm^{-1} , two additional weaker bands in the amide III region centered at 1339 and 1244 cm^{-1} , respectively, and finally two bands centered at 1016 and 854 cm^{-1} .

The weak bands in the amide III were visible in the raw spectra (**Figure 2**) and could easily be observed (without the aid of resolution enhancement techniques) to change in size and shape over time as the dough was mixed. The amide I and II regions were also observed to change in size and shape as the dough was mixed. However, because these regions were highly influenced by the presence of water, the response of protein to mixing could not be easily determined in these regions utilizing the simple technique outlined in this study.

Spectra for each minute within an 8 min mixing cycle of dough displayed a slight offset as the mixing cycle progressed over time to optimum dough development. This offset was displayed throughout the entire mid-IR region ($4000\text{--}700 \text{ cm}^{-1}$). In some cases, the offset itself appeared to increase to an optimum that corresponded to the optimum MT of the dough sample. This offset is likely due to a reflectance scattering effect of the dough sample as each discrete, progressively mixed dough sample became more hydrated with increased mixing, which caused changes in the physical texture of the dough surface. The offset did not appear to influence peak intensity or location.

However, because FT-HATR is highly dependent on the interface between the sample and the HATR sample cell (drier samples making poorer contact with the sample cell surface) and to enhance comparison of the spectra, the spectra were baseline-corrected prior to derivatization to remove this offset as described in the Materials and Methods section of this study.

Previous work by Mathewson (18) gives detailed spectra for the amide III region of a number of various proteins, including gluten. Although the amide III region was of no special interest at the time, protein secondary structure criteria established by the author still made use of bands in this region. According to the criteria of Mathewson, the succinylated form of gluten in solution was predominantly disordered in structure, with some evidence of α -helix and β -sheet. A comparison of spectral data from this study and the work of Mathewson confirmed the existence and location of bands in which we observed α -helix at 1339 cm^{-1} (Mathewson, “none”), α -helix at 1317 cm^{-1} (Mathewson at 1320 cm^{-1}), β -turn at 1285 cm^{-1} (Mathewson at 1289 cm^{-1}), and β -sheet at 1242 cm^{-1} (Mathewson at 1245 cm^{-1}). Although the gluten analyzed by Mathewson was modified (succinylated), the close proximity of the bands that we identified in this study with those from the work of Mathewson demonstrated that the individual bands for identifying protein secondary structural characteristics are essentially constant over a wide variety of protein sources and conditions.

In addition to the confirmation of band location, changes in SDBA were also observed for the five secondary structure bands in dough as it was mixed and scanned through an 8 min mixing cycle. The SDBA at 1339 cm^{-1} (α -helix) showed a decrease in area over time as the dough was mixed and in agreement with the work of Wellner et al. (31). The SDBA at 1317 (α -helix) and 1285 cm^{-1} (β -turn) increased over time, while the SDBA at 1265 cm^{-1} (random coil) decreased over time. While the observed decrease in random coil agrees with previous research (31), the observed increase in β -turn does not. The large SDBA at 1242 cm^{-1} (β -sheet) showed the greatest change and increased over time as the dough was mixed. This observed increase in the β -sheet structure supports the work of Wellner et al. (31), Gilbert et al. (39), and Feeney et al. (40) in which high molecular weight glutenin subunits were observed to increase in β -sheet structure upon hydration. Because the α -helix band at 1339 cm^{-1} decreased in area over time, while the β -sheet band at 1242 cm^{-1} increased, it was reasoned that the

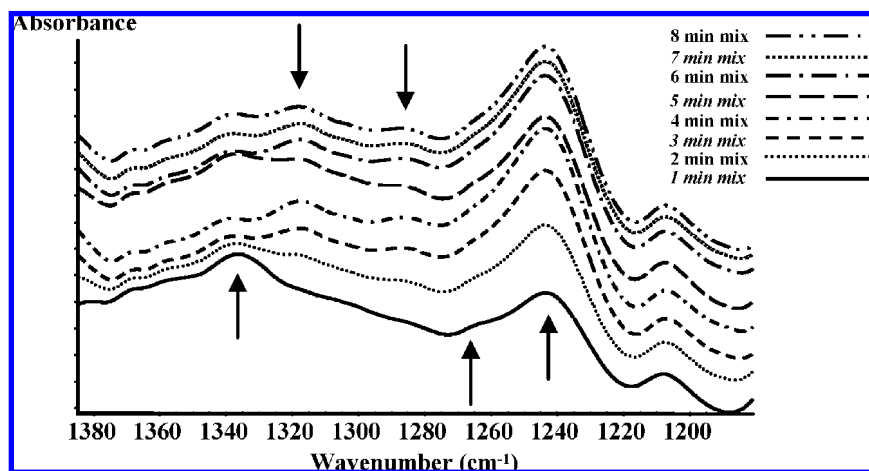


Figure 2. Raw FT-HATR spectra (baseline- and ATR-corrected) of flour–water dough incrementally mixed at 1 min intervals (arrows indicate band areas associated with secondary structure change). Spectra have been graphically arranged (stacked) according to increasing mix time for purposes of illustration.

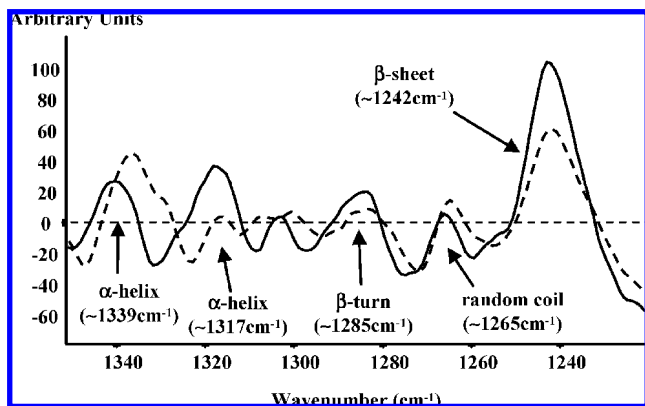


Figure 3. Inverted second derivative (baseline- and ATR-corrected, 11-point smoothed) spectrum in the amide III region ($\sim 1350\text{--}1220\text{ cm}^{-1}$) of flour–water dough mixed for 1 (dashed line) and 4 min (solid line); arrows point to bands associated with specific secondary structure.

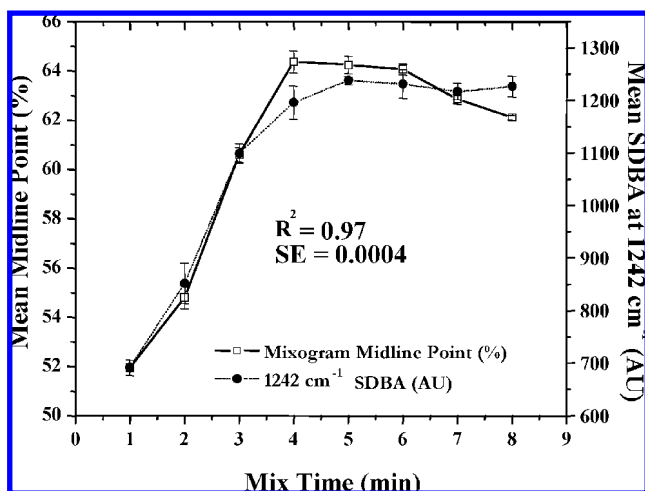


Figure 4. Mean ($n = 3$) mixogram midline point vs mean ($n = 3$) SDBA at 1242 cm^{-1} (β -sheet) for MWG flour–water dough (13% PC and 61% WA, 4.03 min optimum MT) mixed for 8 min.

ratio of the two band areas might possibly provide an accurate approximation of the optimum MT.

On the basis of these observations, the band at 1339 cm^{-1} was tentatively assigned to an α -helix structure, the band at 1317 cm^{-1} also to an α -helix structure, the band at 1285 cm^{-1} to a β -turn structure, the band at 1265 cm^{-1} to a random coil, and the band at 1242 cm^{-1} to a β -sheet structure. **Figure 3** shows the band assignments for the inverted second derivative (baseline- and ATR-corrected, 11-point smoothed) spectrum in the amide III region ($\sim 1350\text{--}1220\text{ cm}^{-1}$) of dough mixed for 1 (dashed line) and 4 min (solid line).

Relationship between Secondary Structure and Dough Rheology. The midline peak time of the digital mixogram is considered an indicator of optimum MT. A comparison of the eight mixogram midline points to the change in SDBA of the MWG dough spectra at each of the five assigned bands described above showed the visual similarity of the spectroscopic method to the traditional mixograph method (**Figure 4**), as well as a point-by-point statistical comparison (coefficient of determination) of the mixogram midline curve to the SDBA curve. A plot of the mean mixogram midline point vs the mean SDBA at 1242 cm^{-1} for the MWG dough is also shown.

Interpretation of **Figure 4** suggests a possible relationship between the spectroscopic data and the mixograph rheological data. Correlation analysis was performed, and the coefficient

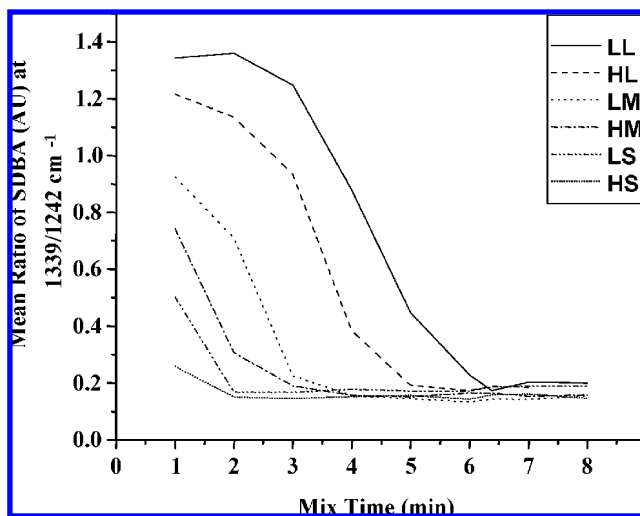


Figure 5. Mean ($n = 3$) ratio of SDBA at $1339/1242\text{ cm}^{-1}$ for the high- and low-PC flour–water doughs from the WQC. LL, low PC and long MT; HL, high PC and long MT; LM, low PC and medium MT; HM, high PC and medium MT; LS, low PC and short MT; and HS, high PC and short MT.

of determination (R^2) and SE of the relationship between change in SDBA over time and the mixogram midline point was calculated for each of the five bands in the mixed dough. The R^2 value for the β -sheet band (1242 cm^{-1}) was 0.97 ($SE = 4.1 \times 10^{-4}\text{ AU}$). R^2 values for the other bands were also high: 0.89 ($SE = 4.0 \times 10^{-3}\text{ AU}$) for the band at 1339 cm^{-1} (α -helix), 0.73 ($SE = 1.0 \times 10^{-3}\text{ AU}$) for the band at 1317 cm^{-1} (α -helix), 0.91 ($SE = 1.0 \times 10^{-4}\text{ AU}$) for the band at 1285 cm^{-1} (β -turn), and 0.86 ($SE = 1.0 \times 10^{-4}\text{ AU}$) for the band at 1265 cm^{-1} (random coil).

To determine if the secondary structure changes initially observed in the MWG dough were the same or similar for other flours with differing optimum MT requirements at similar PC, six flour samples from the WQC were studied and are listed in **Tables 1** and **2**. The originally assigned α -helix band at 1339 cm^{-1} varied somewhat in the study of additional samples at similar PC. Doughs with longer MT requirements had an observed band in this region centered slightly lower than 1339 cm^{-1} (high PC = 1338.2 cm^{-1} and low PC = 1337.7 cm^{-1}), while the doughs with shorter MT requirements had a slightly higher observed band (high PC = 1341.1 cm^{-1} and low PC = 1340.1 cm^{-1}). All other bands for both the high and the low PC flours had bands centered within $<1.0\text{ cm}^{-1}$ of the bands originally assigned.

The optimally mixed doughs for both PC groups (H and L) showed that the band at 1242 cm^{-1} (β -sheet) had the largest SDBA, followed by either the band at 1339 cm^{-1} (α -helix) or the band at 1317 cm^{-1} (α -helix). The band at 1265 cm^{-1} (random coil) had the smallest SDBA. The R^2 values (**Tables 1** and **2**) for the relationship between the SDBA values at the assigned bands and the eight mixogram midline points for the medium and long mixing doughs were high, ranging from 0.69 (“HM” at 1339 cm^{-1}) to 0.99 (“LM” at 1317 cm^{-1} , “HL” at 1285 cm^{-1} , and “LL” at 1242 cm^{-1}). When the R^2 values for each band were averaged, the bands at 1317 (α -helix, mean $R^2 = 0.90$), 1285 (β -turn, mean $R^2 = 0.90$), 1265 (random coil, mean $R^2 = 0.90$), and 1242 cm^{-1} (β -sheet, mean $R^2 = 0.89$) bore the closest relationship to the mixogram midline points, regardless of PC, for the medium and long mixing doughs. The SDBA at 1339 cm^{-1} and the ratio of this area to the SDBA at

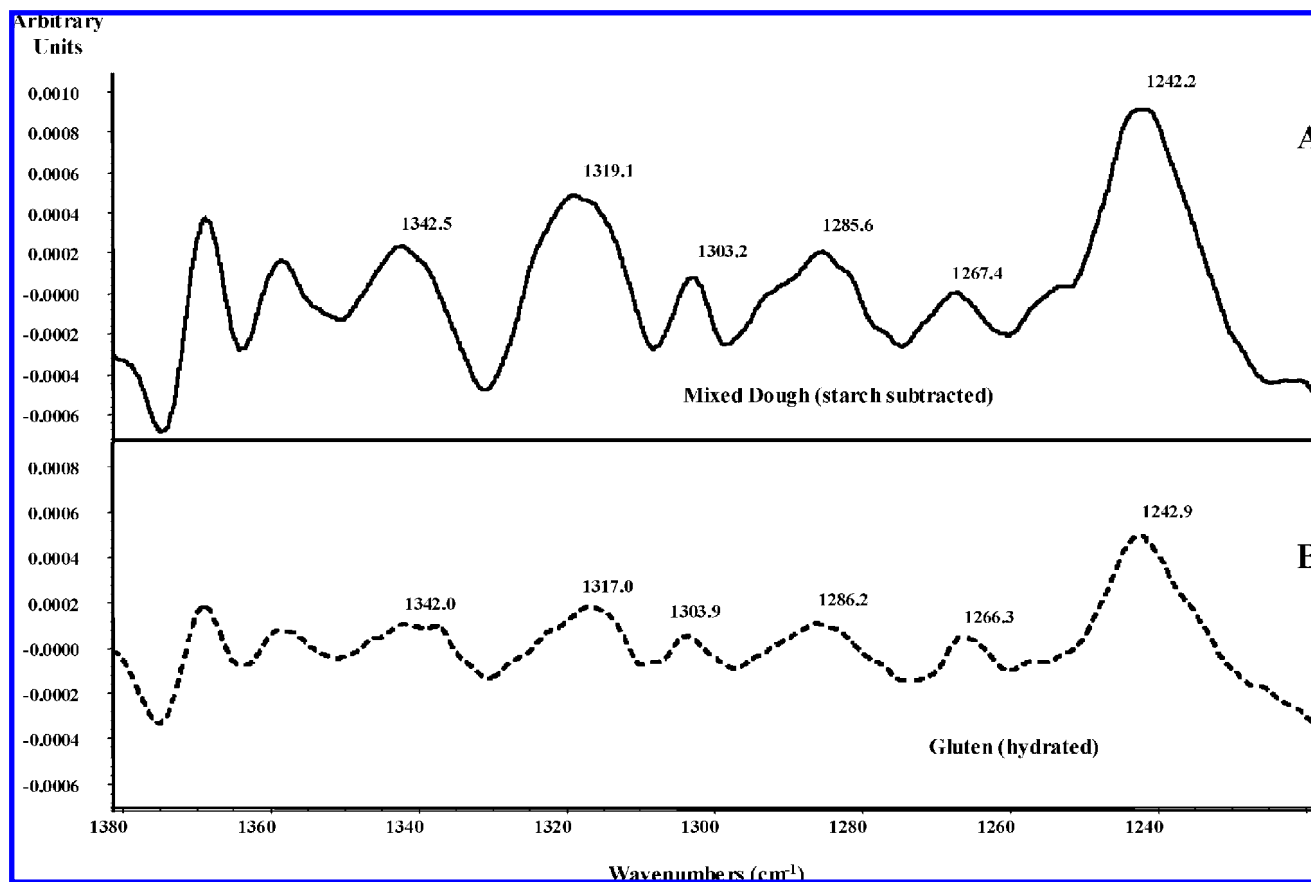


Figure 6. Baseline- and ATR-corrected FT-HATR spectra of (A) mixed flour–water dough after subtraction of isolated starch spectra and (B) hydrated gluten. Spectra have been derivatized (second derivative, five-data point, and two-degree polynomial) and smoothed (11-point, two-degree polynomial Savitsky–Golay function) and then multiplied by a factor of -1 to invert the spectra to locate the bands (upward pointing peaks above the zero line).

1242 cm^{-1} had the lowest mean R^2 values (0.86 and 0.87, respectively).

It can be seen from **Figure 5** that the long mixing flours begin (at 1 min) with the highest SDBA ratio, followed by the medium MT doughs, with the short MT doughs having the lowest 1339/1242 cm^{-1} ratio (α -helix/ β -sheet). This indicates that the β -sheet band areas for the longer mixing doughs were initially much lower at 1 min MT in relation to the α -helix band than for the shorter mixing doughs. This difference is likely due to unique compositional differences in the gluten proteins that allow short MT doughs to more rapidly hydrate and utilize hydrogen bonding (and other noncovalent associations) to develop the secondary structures identified in this study.

FT-HATR analysis during dough mixing revealed direct evidence of changes in band area for five specific bands in the amide III region of the mid-IR as dough was mixed, and these bands have been shown in the literature to be associated with protein secondary structural characteristics. On the basis of these results, the band at 1242 cm^{-1} (β -sheet) was chosen as the recommended band for monitoring dough development due to its large average band area size (greater ease and accuracy of area calculation). The SDBA ratio of 1339/1242 cm^{-1} is also recommended for discriminating differences in MT at a very early stage of dough development (approximately 1 min).

Starch-Subtracted Spectra. Starch is the major constituent of wheat endosperm, comprising roughly 60% of the whole grain composition. To confirm that the identified bands (1339, 1317, 1285, 1265, and 1242 cm^{-1}) truly reflected gluten response to work input and were not a measurement of some unknown (or

as yet unidentified) constituent (e.g., starch), an FT-HATR spectrum of starch isolated from MWG flour was subtracted from the spectra of a fully optimized and developed dough made from MWG flour. **Figure 6A** shows the derivatized and inverted result. An FT-HATR spectrum of fully hydrated gluten, which had been isolated from the same MWG flour, was also collected, and the derivatized and inverted result is shown in **Figure 6B**. It can be seen, then, that both spectra (**Figure 6A,B**) bear very close resemblance to each other. SDBA data for the band areas at 1317, 1285, and 1242 cm^{-1} from starch-subtracted MWG spectra vs the mixogram midline point at each minute of the 8 min mixing cycle were also compared. The R^2 values between these three “starch-subtracted” bands and the mixogram midline were 0.91, 0.95, and 0.93, respectively. These results confirm that the observed spectral response in the amide III region is predominantly due to gluten.

In conclusion, results from this study demonstrate that it is possible to determine the optimum MT of flour–water dough systems by spectroscopic means. Spectroscopic analysis of the doughs in this study showed IR absorption bands associated with α -helix, β -turn, and β -sheet structures that increased in area over time and that the SDBA of these structures reached a peak or plateau that was highly correlated to the optimum MT of the dough as determined by the mixogram midline point. A simultaneous decrease in SDBA of a band associated with random coil structure was observed. The decrease in SDBA for random coil was also highly negatively correlated to the mixogram midline point. Our observation of increasing β -sheet structure with MT confirms earlier work in which β -sheet structures were observed to

be the favored conformation in doughs (29, 41). Thus, as other researchers have suggested, it seems probable that the protein network in a dough system progresses toward a more stabilized and "ordered" state as it is mixed. Because this study showed that the increase in certain protein secondary structures reached an optimum in similar fashion to the mixogram, the data imply that there is an optimal conformation for the gluten macromolecule that is related to optimum viscoelasticity and minimum point of mobility. It is known that protein secondary structures are predominantly stabilized by hydrogen bonding, with specific evidence to gluten proteins demonstrated by Tatham et al. (42), McMaster et al. (43), and Shewry et al. (44). Data from the present study show that certain secondary structures (β -sheet and β -turn in particular) increase during dough mixing. This strongly suggests that hydrogen bonding is therefore an important stabilizing force between protein molecules in the overall gluten network, as it exists in mixed dough.

The results presented in this study show that it is possible, using infrared spectroscopy, to accurately and objectively monitor the rheology of dough systems based on chemical changes in the protein secondary structure of a flour–water system without the need for the more subjective traditional systems that simply measure the physical response of the dough to work input.

ABBREVIATIONS USED

AACC, America Association of Cereal Chemists; ATR, attenuated total reflectance; AU, arbitrary units; FT-IR, Fourier transform infrared; FT-HATR, Fourier transform horizontal attenuated total reflectance; HATR, horizontal attenuated total reflectance; HWWQL, Hard Winter Wheat Quality Laboratory; mb, moisture basis; MCT, mercury cadmium telluride; MT, mix time; MWG, Midwest Grain Inc.; PC, protein content; r , correlation coefficient; R^2 , coefficient of determination; SDBA, second derivative band area; SE, standard error; WA, water absorption; WQC, Wheat Quality Council; ZnSe, zinc selenide.

ACKNOWLEDGMENT

Special thanks to the Wheat Quality Council for flour samples and the U.S. Department of Agriculture, Agricultural Research Service, Hard Winter Wheat Quality Lab (Manhattan, KS), for essential funding.

LITERATURE CITED

- (1) Larsen, R. A. Hydration as a factor in bread flour quality. *Cereal Chem.* **1964**, *41*, 181–187.
- (2) Baig, M. M.; Hoseney, R. C. Effects of mixer speed, dough temperature, and water absorption on flour–water mixograms. *Cereal Chem.* **1977**, *54*, 605–615.
- (3) Kilborn, R. H.; Tipples, K. H. Factors affecting mechanical dough development. I. Effect of mixing intensity and work input. *Cereal Chem.* **1977**, *49*, 34–47.
- (4) Paredes-Lopez, O.; Bushuk, W. Development and "undevelopment" of wheat dough by mixing: physicochemical studies. *Cereal Chem.* **1983**, *60*, 19–23.
- (5) Campos, D. T.; Steffe, J. F.; Ng, P. K. W. Rheological behavior of undeveloped and developed wheat dough. *Cereal Chem.* **1997**, *74* (4), 489–494.
- (6) Lee, L.; Ng, P. K. W.; Whallon, J. H.; Steffe, J. F. Relationship between rheological properties and microstructural characteristics of nondeveloped, partially developed, and developed doughs. *Cereal Chem.* **2001**, *78* (4), 447–452.
- (7) Shewry, P. R.; Tatham, A. S. Disulphide bonds in wheat gluten proteins. *J. Cereal Sci.* **1997**, *25*, 207–227.
- (8) Mecham, D. K.; Cole, E. G.; Sokol, H. A. Modification of flour proteins by dough mixing: Effects of sulfhydryl-blocking and oxidizing agents. *Cereal Chem.* **1963**, *40*, 1–9.
- (9) Tsen, C. C. Effect of oxidizing and reducing agents on changes of flour proteins during dough mixing. *Cereal Chem.* **1969**, *46*, 435–442.
- (10) Bloksma, A. H. Thiol and disulfide groups in dough rheology. *Cereal Chem.* **1975**, *52*, 170r–183r.
- (11) Belitz, H. D.; Kieffer, R.; Seilmeier, W.; Wieser, H. Structure and function of gluten proteins. *Cereal Chem.* **1986**, *63*, 336–341.
- (12) Damodaran, S. Amino acids, peptides, and proteins. In *Food Chemistry*; Fennema, O., Ed.; Marcel Dekker, Inc.: New York, NY, 1996; pp 321–429.
- (13) Aussenac, T.; Carceller, J.; Kleiber, D. Changes in SDS solubility of glutenin polymers during dough mixing and resting (1). *Cereal Chem.* **2001**, *78* (1), 39–45.
- (14) Susi, H. Infrared spectra of biological macromolecules and related systems. In *Structure and Stability of Biological Macromolecules*; Timasheff, S.; Fasman, G., Eds.; Marcel Dekker, Inc.: New York, NY, 1969; pp 575–663.
- (15) Burno, T. J.; Svoronos, P. D. N. Infrared spectrophotometry. *CRC Handbook of Fundamental Spectroscopic Correlation Charts*; CRC Taylor & Francis Group: New York, NY, 2006; pp 17–84.
- (16) Singh, B. R.; DeOliveira, D. B.; Fu, F. N.; Fuller, M. P. Fourier transform infrared 15N analysis of amide III bands of proteins for the secondary structure estimation. Proceedings of Biomolecular Spectroscopy III, Jan 17–18, 1993, Los Angeles, CA, pp 47–55.
- (17) Shouwei, C.; Singh, B. R. A distinct utility of the amide III infrared band for secondary structure estimation of aqueous protein solutions using partial least squares. *Biochemistry* **2004**, *43*, 2541–2549.
- (18) Cai, S.; Singh, B. R. Identification of beta-turn and random coil amide III infrared bands for secondary structure estimation of proteins. *Biophys. Chem.* **1999**, *80*, 7–20.
- (19) Mathewson, P. R. Fourier transform infrared spectroscopic analysis of protein secondary structure. Development of Enzymological and Fourier transform Infrared Spectroscopic Methods for Analysis of Proteolytic Activity; Ph.D. Thesis, Kansas State University, Manhattan, KS, 1985; pp 96–224.
- (20) Dousseau, F.; Pézolet, M. Determination of the secondary structure of proteins in aqueous solutions from amide I and amide II infrared bands. Comparison between classical and partial least-square methods. *Biochemistry* **1990**, *29*, 8771–8779.
- (21) Kaiden, K.; Matsui, T.; Tanaka, S. A study of the amide III band by FT-IR spectrometry of the secondary structure of albumin, myoglobin, and gamma-globulin. *Appl. Spectrosc.* **1987**, *41*, 180–184.
- (22) He, W. Z.; Newell, W. R.; Haris, P. I.; Chapman, D.; Barber, J. Protein secondary structure of the isolated photosystem II reaction center and conformational changes studied by Fourier transform infrared spectroscopy. *Biochemistry* **1991**, *30*, 4552–4559.
- (23) Pribic, R.; van Stokkum, I. H. M.; Chapman, D.; Haris, P. I.; Bloemdal, M. Protein secondary structure from Fourier transform infrared and/or circular dichroism spectra. *Anal. Biochem.* **1993**, *214*, 366–378.
- (24) Singh, B. R.; Fuller, M. P.; Schiavo, G. Molecular structure of tetanus neurotoxin as revealed by Fourier transform infrared and circular dichroic spectroscopy. *Biophys. Chem.* **1990**, *36*, 155–166.
- (25) Fu, F. D.; DeOliveira, D. B.; Trumble, W. R.; Sarkar, H. K.; Singh, B. R. Secondary structure estimation of proteins using the amide III region of Fourier transform infrared spectroscopy: Application to analyze calcium-binding-induced structural changes in calyculin A. *Appl. Spectrosc.* **1994**, *48*, 1432–1441.
- (26) Fu, K.; Griebenow, K.; Hsieh, L.; Klibanov, A. M.; Langer, R. FTIR characterization of the secondary structure of proteins encapsulated within PLGA microspheres. *J. Controlled Release* **1999**, *58*, 357–366.

- (27) Costantino, H. R.; Schwendeman, S. P.; Griebenow, K.; Klibanov, A. M.; Langer, R. On the secondary structure and aggregation of lyophilized tetanus toxoid. *J. Pharm. Sci.* **1996**, *85*, 1290–1293.
- (28) Costantino, H. R.; Andya, J. D.; Shire, S. J.; and Hsu, C. C. Fourier-transform infrared spectroscopic analysis of the secondary structure of recombinant humanized immunoglobulin G. *J. Pharm. Sci.* **1997**, *3*, 121–128.
- (29) Pezolet, M.; Bonenfant, S.; Dousseau, F.; Popineau, Y. Conformation of wheat gluten proteins. Comparison between functional and solution states as determined by infrared spectroscopy. *Fed. Eur. Biochem. Soc. Lett.* **1992**, *299*, 247–250.
- (30) Seabourn, B. W. Determination of protein secondary structure in wheat flour-water systems during mixing using Fourier transform horizontal attenuated total reflectance infrared spectroscopy. Ph.D. Thesis, Kansas State University, 2002; pp 1–151.
- (31) Wellner, N.; Mills, E. N. C.; Brownsney, G.; Wilson, R. H.; Brown, N.; Freeman, J.; Halford, N. G.; Shewry, P. R.; Belton, P. S. Changes in protein secondary structure during gluten deformation studied by dynamic Fourier transform infrared spectroscopy. *Biomacromolecules* **2005**, *6*, 255–261.
- (32) Bruun, S. W.; Sondergaard, I.; Jacobsen, S. Analysis of protein structures and interactions in complex food by near-infrared spectroscopy. 1. Gluten powder. *J. Agric. Food Chem.* **2007**, *55*, 7234–7243.
- (33) Bruun, S. W.; Sondergaard, I.; Jacobsen, S. Analysis of protein structures and interactions in complex food by near-infrared spectroscopy. 2. Hydrated gluten. *J. Agric. Food Chem.* **2007**, *55*, 7244–7251.
- (34) American Association of Cereal Chemists. *Approved Methods of the AACC*, 10th ed.; The Association: St. Paul, MN, 2000.
- (35) Nunn, S.; Nishikida, K. Advanced ATR Correction Algorithm; Thermo Electron Corporation Application Note; Thermo Electron Corporation: Madison, WI, 2003.
- (36) Susi, H.; Byler, D. M. Protein structure by Fourier transform infrared spectroscopy: second derivative spectra. *Biochem. Biophys. Res. Commun.* **1983**, *115*, 391–397.
- (37) Savitsky, A.; Golay, M. J. E. Smoothing and differentiation of data by simplified least squares procedures. *Anal. Chem.* **1964**, *36*, 1627–1639.
- (38) Krimm, S.; Bandekar, J. Vibrational spectroscopy and conformation of peptides, polypeptides, and proteins. *Adv. Protein Chem.* **1986**, *38*, 181–364.
- (39) Gilbert, S. M.; Wellner, N.; Belton, P. S.; Greenfield, J. A.; Siligardi, G.; Shewry, P. R.; Tatham, A. S. Related expression and characterisation of a highly repetitive peptide derived from a wheat seed storage protein. *Biochim. Biophys. Acta* **2000**, *1479* (1–2), 135–146.
- (40) Feeney, K. A.; Wellner, N.; Gilbert, S. M.; Halford, N. G.; Tatham, A. S.; Shewry, P. R.; Belton, P. S. Molecular structures and interactions of repetitive peptides based on wheat glutenin subunits depend on chain length. *Biopolymers* **2003**, *72*, 123–131.
- (41) Popineau, Y.; Bonenfant, S.; Cornec, M.; Pezolet, M. A study by infrared spectroscopy of the conformations of gluten proteins differing in their gliadin and glutenin compositions. *J. Cereal Sci.* **1994**, *20*, 15–22.
- (42) Tatham, A. S.; Drake, A. F.; Shewry, P. R. A conformational study of a glutamine- and proline-rich cereal seed protein, C hordein. *Biochem. J.* **1985**, *1226* (2), 557–562.
- (43) McMaster, T. J.; Miles, M. J.; Kasarda, D. D.; Shewry, P. R.; Tatham, A. S. Atomic force microscopy of A-gliadin fibrils and in situ degradation. *J. Cereal Sci.* **1999**, *31*, 281–286.
- (44) Shewry, P. R.; Halford, N. G.; Belton, P. S.; Tatham, A. S. The structure and properties of gluten: an elastic protein from wheat grain. *Phil. Trans. R. Soc. London B* **2002**, *357*, 133–142.

Received for review December 10, 2007. Revised manuscript received March 7, 2008. Accepted March 19, 2008.

JF703569B